

Nuclear magnetic resonance linewidth and spin diffusion in ^{29}Si isotopically controlled silicon

Hiroshi Hayashi and Kohei M. Itoh*

Department of Applied Physics and Physico-Informatics, Keio University, 3-14-1 Hiyoshi, Kohoku-ku, Yokohama 223-8522, Japan

Leonid S. Vlasenko

A. F. Ioffe Physico-Technical Institute, 194021 Saint Petersburg, Russia

(Received 21 February 2008; revised manuscript received 3 September 2008; published 6 October 2008)

A nuclear magnetic resonance (NMR) study was performed with n -type silicon single crystals containing ^{29}Si isotope abundance f ranges from 1.2% to 99.2%. The nuclear spin diffusion coefficient D has been determined from the linewidth of significantly enhanced ^{29}Si NMR signals utilizing a developed dynamic nuclear polarization (DNP) method. The ^{29}Si NMR linewidth depends linearly on f , at least when $f < 10\%$, and approaches $\propto f^{1/2}$ dependence when $f > 50\%$. The estimated ^{29}Si nuclear spin diffusion time T_{sd} between phosphorus atoms used for DNP is more than ten times shorter than the nuclear polarization time T_1^p of ^{29}Si nuclei around phosphorus. Therefore, the regime of “rapid spin diffusion” is realized in the DNP experiments.

DOI: [10.1103/PhysRevB.78.153201](https://doi.org/10.1103/PhysRevB.78.153201)

PACS number(s): 75.40.Gb, 28.60.+s, 76.60.-k, 76.70.Fz

The advantages in the availability of silicon based structures with controlled isotope positioning¹⁻⁴ provide an opportunity for future applications of these semiconductor materials for spin electronics and quantum computing.^{5,6} This stimulated magnetic resonance investigations including nuclear magnetic resonance (NMR),⁷ optical nuclear polarization,⁸ and dynamic nuclear polarization (DNP)^{9,10} in isotopically controlled silicon crystals. Nuclear spin diffusion plays an important role in all these phenomena to transfer the nuclear spin polarization from the local paramagnetic centers to the whole crystal volume.

The concept of nuclear spin diffusion was introduced by Bloembergen¹¹ to explain several orders of disagreement between theoretical and experimental values of the nuclear spin-lattice relaxation time T_1 in crystals containing paramagnetic centers. The origin of spin diffusion is a dipolar coupling between nuclear magnetic moments. For two nuclear spins, I_i and I_j , separated by distance r_{ij} , the Hamiltonian H_{dd} is given by

$$H_{\text{dd}} = d_{ij}[4I_{iz}I_{jz} - (I_{i+}I_{j-} + I_{i-}I_{j+})], \quad (1)$$

where I_z is the z component of the angular momentum operator, and I_+ and I_- are the raising and lowering operators, respectively. The coefficient d_{ij} is given by

$$d_{ij} = \frac{\gamma^2 \hbar^2}{4|r_{ij}|^3}(1 - 3 \cos^2 \theta_{ij}), \quad (2)$$

where γ is the nuclear gyromagnetic ratio, $\hbar = h/2\pi$ is Planck's constant, and θ_{ij} is the angle between the vector r_{ij} and the direction of the magnetic field.

The energy conserving mutual flip-flop transitions between antiparallel nuclear spins caused by terms $I_{i+}I_{j-}$ and $I_{i-}I_{j+}$ in Eq. (1) are responsible for nuclear spin diffusion. The same interactions described by Hamiltonian (1) provide the contribution to the NMR linewidth $\Delta\nu_{\text{dd}}$ and determine the nuclear spin-spin relaxation time $T_2 \approx 1/\Delta\nu_{\text{dd}}$.

The spin diffusion coefficient is given as¹¹

$$D = a^2 W_{12}, \quad (3)$$

where a is the average distance between two neighboring nuclei and W_{12} is the probability of the flip-flop transition, which can be relatively large for the neighboring nuclei. W_{12} is of the order of $1/T_2$. Because the time T_2 is determined by interactions not only between neighboring nuclei but also with the distant nuclei, D is often described by the following approximate relation:¹²

$$D \approx \frac{1}{30T_2} a^2 \approx \frac{\Delta\nu_{\text{dd}}}{30} a^2. \quad (4)$$

Various theoretical calculations of nuclear spin diffusion based on density-matrix technique,¹³ on the calculation of higher moments of a resonance line,¹⁴ on the statistical mechanics of irreversible processes,¹⁵ and on classical spin dynamics¹⁶ have been performed. Direct experimental determination of D is limited by the difficulty to create the spatial gradient of the magnetization on the diffusion length $L \approx \sqrt{DT_1}$. Zhang and Cory¹⁷ successfully made a direct measurement of the spin diffusion rate in CaF_2 single crystal using incoherent NMR scattering measurements, showing good agreement with theoretical predictions. However, indirect determination of D from time T_2 is reliable when dipolar interactions dominate.

DNP is a useful tool for the investigation of nuclear spin properties through NMR. DNP in silicon has been carried out recently in lower-temperature and higher-magnetic-field regions to achieve high nuclear polarization.^{8,18} This Brief Report describes experiments on detecting NMR signals enhanced strongly by a developed DNP technique in silicon single crystals containing different percentages of ^{29}Si isotope f . The analysis of the NMR linewidth with respect to estimation of the diffusion coefficient according to Eq. (4) will be given. Experimental results will be discussed with theoretical calculations of the resonance line shape,^{19,20} linewidth,²⁰ and diffusion coefficient²¹ as functions of f using statistical methods for disordered or randomly distributed magnetic moments.

The experiments were performed with n -type silicon

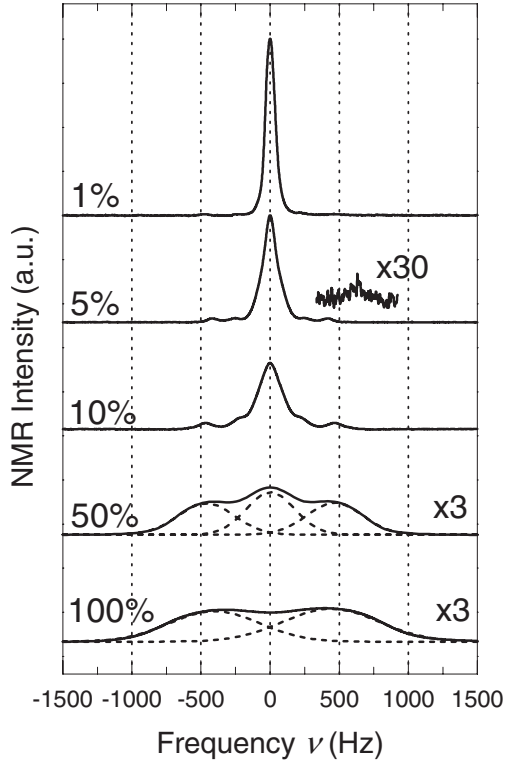


FIG. 1. The DNP enhanced ^{29}Si NMR spectra detected in isotopically controlled silicon single crystals for orientation of the magnetic field approximately along $[111]$ crystal axis. The horizontal axis is offset by ^{29}Si nuclear Larmor frequency of 60 MHz; the vertical axis is arbitrary. The thermal equilibrium signal in a ^{29}Si -5% sample is also shown (horizontal axis is arbitrarily shifted). The dotted curves in the ^{29}Si -50% and 100% samples indicate the components of absorption curve obtained by fitting it with multiple Gaussian curves. The total area under the NMR spectra is normalized to be unity (but multiplied to present their shapes clearly).

single crystals containing ^{29}Si isotopic abundance f of 1.2%, 4.7%, 10.3%, 47.9%, and 99.2% with the phosphorus concentrations $N_{\text{d}}=(0.6-1.6)\times 10^{15}\text{ cm}^{-3}$ (referred in this text as ^{29}Si -1%, 5%, 10%, 50%, and 100% samples, respectively). The weak ^{29}Si NMR signals were enhanced by DNP performed in an EPR JEOL JES-RE3X X-band continuous-wave spectrometer. One of the two phosphorus EPR lines was saturated by a 200-mW microwave field at 12 K.⁹ After 20 h of saturation, the sample was transferred to a Chemagnetics CMX300 CP/MAS-NMR spectrometer where the ^{29}Si NMR signal was detected at room temperature and a magnetic field of 7 T. The absorption spectrum was acquired after Fourier transformation of the free-induction decay signal following a $\pi/2$ pulse. The pulse length and acquisition delay time were 9 and 35 μs , respectively. The extremely long T_1 for all investigated samples ($T_1 \approx 3$ h at room temperature²²) allowed us to transfer the samples without losing nuclear magnetization.

Typical DNP enhanced ^{29}Si NMR spectra are shown in Fig. 1. The thermal equilibrium signal for the ^{29}Si -5% sample detected after 66 h relaxation at room temperature and 7 T is also shown to illustrate the efficiency of DNP. As shown in the theoretical calculations of the resonance line,²⁰

TABLE I. Experimentally determined square root of the second moment (in hertz) and the ratio of the higher-order moment to the second moment of the NMR absorption line. Ratios expected for different line shapes are shown for comparison.

Sample	$M_2^{1/2}$	M_4/M_2^2	M_6/M_2^3	M_8/M_2^4
^{29}Si -1%	61.1	11.1	259	7640
^{29}Si -5%	127	7.28	79.9	1010
^{29}Si -10%	204	4.67	31.6	258
^{29}Si -50%	436	2.66	12.8	99.3
^{29}Si -100%	552	2.52	11.2	74.2
Lorentzian limit		∞	∞	∞
Gaussian		3	15	105
Rectangular		1.8	3.9	9.0
Pair limit		1	1	1

line shape, and width of the DNP enhanced NMR spectra show a strong dependence on the amount of ^{29}Si isotope f and provide a clear observation of the satellite peaks, so-called Pake's doublet, arising from the nearest-neighbor ^{29}Si nuclei even in a naturally abundant ^{29}Si -5% sample which contains only $f^2=0.22\%$ of the ^{29}Si pairs in the silicon matrix. In addition, the positions of the satellite peaks depend on the crystal orientation in the external magnetic field described by Eq. (2).^{7,23} Although the lines have a partially overlapped structure, the components of the absorption curve in ^{29}Si -50% and 100% samples are Gaussian and well fitted with multiple Gaussian curves.

The method of moments developed by Van Vleck²⁴ is often used for the analysis of the resonance line shape. The $2n$ th moment M_{2n} and the ratio of the higher-order moment to the second moment M_{2n}/M_2^n are commonly used as standard parameters for the characterization.¹⁹ A sharp doublet peak (two δ functions at $\nu=\pm M_2^{1/2}$) corresponds to $M_{2n}/M_2^n=1$ (pair limit), while the double peak merges into a single peak when $M_4/M_2^2 \geq 2.85$. Gaussian line shape has $M_4/M_2^2=3$. For a narrow line shape with longer wings, such as a Lorentzian, $M_{2n}/M_2^n \rightarrow \infty$ (Lorentzian limit). The spectral moments were numerically calculated from the experimental NMR lines (Table I). We can quantitatively see how the NMR line shape varies from a single Lorentzian in a ^{29}Si -1% sample to a double peak in a ^{29}Si -100% sample with an increase in ^{29}Si abundance. It should be noted that the analysis of the linewidth using the second and fourth moments of the Gaussian and Lorentzian line shapes shows the linear dependence of linewidth on f when $f < 1\%$ and square-root dependence when $f > 10\%$.²⁵

To estimate the linewidths $\Delta\nu$ of the detected NMR signals of the complex line shapes, we used the values of $\Delta\nu$ determined in Ref. 20 as

$$\Delta\nu = 1/F(0), \quad (5)$$

where $F(0)$ is the value of the normalized line-shape function $F(\nu)$ taken at the center of the NMR line ($\nu=0$ Hz). The NMR linewidths $\Delta\nu$ obtained by this method from the experimentally observed signals at the orientation of the mag-

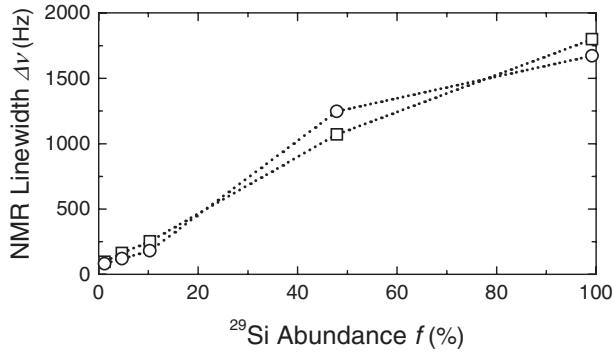


FIG. 2. Dependence of the NMR linewidth $\Delta\nu$ determined by Eq. (5) (squares) and FWHM (circles) on the ^{29}Si isotope abundance f .

netic field approximately along [111] crystal axis are plotted in Fig. 2 as a function of f (squares). The full widths at half maximum (FWHM) measured directly from the NMR lines are also plotted in Fig. 2 (circles).

The NMR linewidth due to the dipole-dipole interaction between nuclear magnetic moments should vanish at infinite nuclear spin spacing r_{ij} . However, $\Delta\nu$ goes to a nonzero value of ~ 70 Hz at $f=0\%$ (see Fig. 2). The remaining linewidth of 70 Hz shows some additional contribution to FWHM, such as inhomogeneity of the external magnetic field over the sample and a nonzero delay time of the NMR spectrometer when the strongest part of the free-induction decay signal is lost. To obtain the contribution to linewidth purely due to the dipole-dipole interaction, $\Delta\nu_{\text{dd}}$, the value of 70 Hz was subtracted from $\Delta\nu$. The dependence of the $\Delta\nu_{\text{dd}} = \Delta\nu - 70$ Hz on f is shown in Fig. 3. These results show that $\Delta\nu_{\text{dd}}$ determined by different methods linearly depends on f when $f < 10\%$ and changes to square-root dependence when $f > 50\%$, which is in good agreement with the theoretical calculations of the linewidth in the system of randomly distributed spins.²⁰

In addition, we estimated the nuclear diffusion coefficient D using Eq. (4) and values of $\Delta\nu_{\text{dd}}$. The average distance between ^{29}Si nuclei a can be found from the relation,

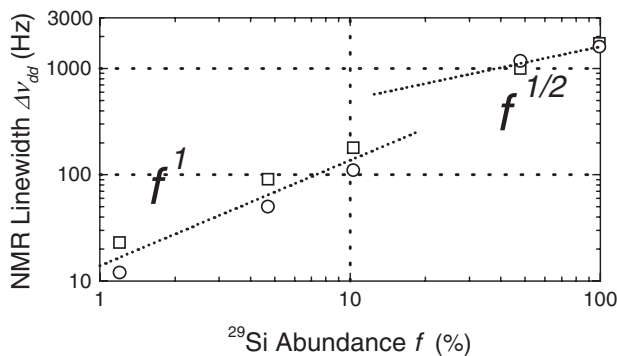


FIG. 3. Dependence of the NMR linewidth due to the dipole-dipole interaction, $\Delta\nu_{\text{dd}}$, determined by Eq. (5) (squares) and FWHM (circles) on the ^{29}Si isotope abundance f . The dashed lines show the linear and square-root dependences.

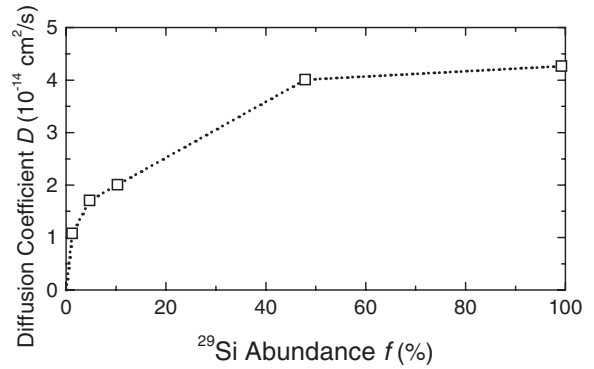


FIG. 4. Dependence of the ^{29}Si nuclear-spin-diffusion coefficient D on the ^{29}Si isotope abundance f .

$$a \approx N_N^{-1/3} = \left(f \frac{8}{d^3} \right)^{-1/3}, \quad (6)$$

where N_N is the ^{29}Si concentration, 8 is the number of atoms in a unit cell of diamond structure, and $d=0.543$ nm is the lattice constant of silicon. The dependence of D on f is shown in Fig. 4. The $\Delta\nu_{\text{dd}}$ values were taken using Eq. (5). A monotonous increase in D with an increase in f and a slow increase at higher abundance is in qualitative agreement with the theoretical simulation of spin diffusion in a disordered spin system.²¹ Similar dependence of D on f was found for the FWHM estimations.

Using the values of D , the diffusion time T_{sd} of the nuclear polarization transfer on the distance of $L=R/2$ between paramagnetic centers can be found,

$$T_{\text{sd}} \approx \frac{L^2}{D} = \frac{R^2}{4D}, \quad (7)$$

where $R \approx N_d^{-1/3}$ is the average distance between phosphorus atoms. The distances a and L , and time T_{sd} for the investigated samples are summarized in Table II.

The time T_{sd} can be compared with the nuclear spin polarization time T_1^p obtained from the exponential growth of ^{29}Si NMR signals in the DNP experiments and are also listed in Table II. The time T_{sd} is much shorter than the nuclear polarization time showing the fast ^{29}Si nuclear spin diffusion between the phosphorus paramagnetic centers. Together with the observed exponential increase in the nuclear polarization with the saturation time, it allows us to conclude that the

TABLE II. The average distance between ^{29}Si nuclei a (\AA), average half distance between phosphorus donors L (\AA), nuclear spin diffusion time T_{sd} (hours), and nuclear spin polarization time T_1^p (hours) in the investigated samples.

Sample	a	L	T_{sd}	T_1^p
^{29}Si -1%	12	560	0.82	73.5
^{29}Si -5%	7.5	540	0.47	19.5
^{29}Si -10%	5.8	430	0.25	4.5
^{29}Si -50%	3.5	590	0.24	8.8
^{29}Si -100%	2.7	540	0.19	9.3

case of rapid nuclear spin diffusion regime^{12,26–28} is realized in all investigated samples.

In summary, the analysis of the ²⁹Si NMR linewidth in the silicon crystals containing different amounts of the ²⁹Si isotope showed that the NMR linewidth is proportional to f when $f < 10\%$ and approaches square-root dependence on f when $f > 50\%$. The nuclear spin diffusion coefficient D increased from 1×10^{-14} to 4×10^{-14} cm²/s. The nuclear-spin diffusion between phosphorus atoms is more than ten times faster than the increase in the ²⁹Si nuclear polarization around phosphorus atoms in the DNP experiments corre-

sponding to the regime of the rapid spin diffusion.

We thank T. Itahashi for all the helpful experimental support. We also thank Central Service Facilities for Research at Keio University for the provision of the well-developed experimentation environment. This work was supported in part by Grant-in-Aid for Scientific Research by MEXT Specially Promoted Research No. 18001002, by Special Coordination Funds for Promoting Science and Technology, and by Grant-in-Aid for the Global Center of Excellence at Keio University.

*kitoh@appi.keio.ac.jp

- ¹K. Takyu, K. M. Itoh, K. Oka, N. Saito, and V. I. Ozhogin, *Jpn. J. Appl. Phys., Part 2* **38**, L1493 (1999).
- ²T. Kojima, R. Nebashi, K. M. Itoh, and Y. Shiraki, *Appl. Phys. Lett.* **83**, 2318 (2003).
- ³K. M. Itoh, J. Kato, F. Uemura, A. K. Kaliteyevskii, O. N. Godisov, G. G. Devyatych, A. D. Bulanov, A. V. Gusev, I. D. Kovalev, P. G. Sennikov, H.-J. Pohl, N. V. Abrosimov, and H. Riemann, *Jpn. J. Appl. Phys., Part 1* **42**, 62481 (2003).
- ⁴T. Sekiguchi, S. Yoshida, and K. M. Itoh, *Phys. Rev. Lett.* **95**, 106101 (2005).
- ⁵T. D. Ladd, J. R. Goldman, F. Yamaguchi, Y. Yamamoto, E. Abe, and K. M. Itoh, *Phys. Rev. Lett.* **89**, 017901 (2002).
- ⁶K. M. Itoh, *Solid State Commun.* **133**, 747 (2005).
- ⁷A. S. Verhulst, D. Maryenko, Y. Yamamoto, and K. M. Itoh, *Phys. Rev. B* **68**, 054105 (2003).
- ⁸A. S. Verhulst, I. G. Rau, Y. Yamamoto, and K. M. Itoh, *Phys. Rev. B* **71**, 235206 (2005).
- ⁹H. Hayashi, W. Ko, T. Itahashi, A. Sagara, K. M. Itoh, L. S. Vlasenko, and M. P. Vlasenko, *Phys. Status Solidi C* **3**, 4388 (2006).
- ¹⁰L. S. Vlasenko, M. P. Vlasenko, D. S. Poloskin, R. Laiho, H. Hayashi, T. Itahashi, A. Sagara, and K. M. Itoh, *Phys. Status Solidi C* **3**, 4376 (2006).
- ¹¹N. Bloembergen, *Physica (Amsterdam)* **15**, 386 (1949).
- ¹²G. R. Khutsishvili, *Sov. Phys. Usp.* **8**, 743 (1966).
- ¹³I. J. Lowe and S. Gade, *Phys. Rev.* **156**, 817 (1967).
- ¹⁴A. G. Redfield and W. N. Yu, *Phys. Rev.* **169**, 443 (1968).
- ¹⁵P. Borckmans and D. Walgraef, *Phys. Rev.* **167**, 282 (1968).
- ¹⁶C. Tang and J. S. Waugh, *Phys. Rev. B* **45**, 748 (1992).
- ¹⁷W. Zhang and D. G. Cory, *Phys. Rev. Lett.* **80**, 1324 (1998).
- ¹⁸A. E. Dementyev, D. G. Cory, and C. R. Ramanathan, *Phys. Rev. Lett.* **100**, 127601 (2008).
- ¹⁹G. W. Parker and F. Lado, *Phys. Rev. B* **8**, 3081 (1973).
- ²⁰C. W. Myles, C. Ebner, and P. A. Fedders, *Phys. Rev. B* **14**, 1 (1976).
- ²¹I. M. Nolden and R. J. Silbey, *Phys. Rev. B* **54**, 381 (1996).
- ²²R. G. Shulman and B. J. Wyluda, *Phys. Rev.* **103**, 1127 (1956).
- ²³L. S. Vlasenko, *Sov. Phys. Tech. Phys.* **10**, 467 (1984).
- ²⁴J. H. Van Vleck, *Phys. Rev.* **74**, 1168 (1948).
- ²⁵C. Kittel and E. Abrahams, *Phys. Rev.* **90**, 238 (1953).
- ²⁶W. E. Blumberg, *Phys. Rev.* **119**, 79 (1960).
- ²⁷A. Abragam, *The Principles of Nuclear Magnetism* (Oxford University Press, New York, 1961).
- ²⁸C. D. Jeffries, *Dynamic Nuclear Orientation* (Wiley, New York, 1963).